Excitation Dynamics in the Core Antenna in the Photosystem I Reaction Center of the Chlorophyll *d*-Containing Photosynthetic Prokaryote *Acaryochloris marina*

Dehui Mi,[†] Min Chen,[‡] Su Lin,[†] Michael Lince,[†] Anthony W. D. Larkum,[‡] and Robert E. Blankenship*[,†]

Department of Chemistry and Biochemistry, Arizona State University, Tempe, Arizona 85287-1604, and School of Biological Sciences, A08, University of Sydney, Sydney, NSW 2006, Australia

Received: August 25, 2002; In Final Form: December 1, 2002

Transient absorption difference spectroscopy on the picosecond time scale was used to study the ultrafast excitation dynamics in the photosystem I core antenna in *Acaryochloris marina*, a newly discovered marine oxygenic photosynthetic prokaryote that contains chlorophyll *d* as its major photopigment. Photosystem I particles were isolated using a detergent treatment of the thylakoid membranes and sucrose gradient ultracentrifugation. Steady-state fluorescence measurements at both room temperature and 77 K as well as ultrafast transient absorbance and fluorescence measurements were carried out on photosystem I. For ultrafast transient absorbance measurements, the sample was excited at 720, 740, and 745 nm with either high or low excitation energy. In each case, after a rapid (subpicosecond) energy transfer, the excitation energy resided on pigments absorbing at 710 nm. A kinetic component of about 40 ps and a nondecaying component on the order of nanoseconds were resolved. The 40-ps component was assigned to the trapping of excitation energy into the reaction center. The trapping time was confirmed by time-resolved fluorescence measurements. The 40-ps trapping time, because of the formation of a charge-separated state in the reaction center, is nearly excitation wavelength-independent. Narrow spectral-band excitations (5-nm fwhm) at 690, 720, 730, and 740 nm were used to excite different pools of the photosystem I core antenna selectively. The initial spectral changes show a strong excitation wavelength dependence. An exceptionally broad, prompt bleaching, spanning from 700 to 740 nm, was induced when excitation was directly into the primary electron donor, P740, suggesting the existence of an excitonic coupling between a group of pigments, most likely the reaction center cofactors. A 2−3-ps energy equilibration process was also observed, similar to that observed in other cyanobacterial photosystem I. No evidence was found for a pool of long-wavelength antenna pigments with energy lower than that of the primary donor P740.

Introduction

Cyanobacteria are a large and diverse group of oxygenic photosynthetic prokaryotes.[1,2] This large phylum includes three groups that share similarities according to 16S rRNA analysis:[3] authentic cyanobacteria (containing chl *a*), prochlorophytes (containing both chl *a* and chl *b*), and the newly discovered *Acaryochloris marina* (containing both chl *d* and chl *a*).[4] *A. marina* appears to fall within the cyanobacterial radiation in overall properties. However, *A. marina* is unique among photosynthetic organisms because chl *d* is its principal photopigment, although small amounts of chl *a* are also present.[5]

Photosystem I is a multisubunit pigment−protein complex in all oxygenic photosynthetic organisms.[6] The latest structural information on photosystem I is the crystal structure of the cyanobacterium *Synechococcus elongatus* at a resolution of 2.5 Å.[7] It reveals 12 protein subunits, 127 cofactors including 96 chlorophylls, 2 phylloquinones, 3 Fe_4S_4 clusters, 22 carotenoids, and 4 lipids. In the photosystem I structural model, the chlorophyll pigments, including both the antenna chlorophylls and the chlorophylls involved in the electron transfer within the reaction center, exist in clusters linked by one or two chlorophyll molecules.[7,8] The majority of the pigments constitute an antenna system.[9,10] The antenna absorbs light and funnels the excitations to the central core of the complex where electron transfer takes place.[11] When a photosystem I complex is excited, an excitation equilibration between all of the spectral forms of chlorophyll takes place within several picoseonds.[9,10] After that process is complete, the excitation energy is trapped into the reaction center at a much slower rate. This trapping process takes 20−40 ps depending on the species.[9,10] Among all of the antenna chlorophylls, the so-called red pigments are especially interesting. They absorb at wavelengths longer than that of the special pair and contribute to the energy-trapping process, although their precise functional role is not well understood.[9,10,12−14] Their special properties are thought to be due to both pigment−protein and pigment−pigment interactions and possible dimer formation.

A. marina has aroused great interest since its discovery, largely because of its unique pigment composition.[4,5,15] Similar to authentic cyanobacteria, *A. marina* contains two photosystems. Chlorophyll *d* serves as a light-harvesting pigment for both photosystem II and photosystem I.[15,16] A trace amount of chl *a* is also found in *A. marina* and appears to be localized mostly in photosystem II. The ratio chl *d*/chl *a* depends on the growth conditions.[26] Phycobilins (phycocyanin) are present, although there are no visible phycobilisomes.[17,18] The major chlorophyll-containing light-harvesting complex is believed to be similar to that of a pcb-type protein.[19]

* Corresponding author. E-mail: Blankenship@asu.edu.
[†] Arizona State University.
[‡] University of Sydney.

10.1021/jp0268260 CCC: $25.00
Published on Web 01/15/2003

Chl *d* is the dominant chlorophyll both in the antenna and in the special pair in photosystem I. The photosystem I complex involving chl *d* was purified and found to have Psa A-F, -L, -K, and two extra polypeptides.[20] Instead of P700 as the primary donor for photosystem I, *A. marina* has P740.[20] The antenna size of photosystem I was estimated to be 80−90 chl *d* including 3−10 molecules absorbing at 735 nm.[16] However, the number of chl *d* molecules per photosystem I was determined to be 145 ± 8 by Hu et al.,[20] and this discrepancy remains to be resolved. Chlorophyll *a* was undetectable in photosystem I. [20]

The midpoint potential of P740/P740$^+$ (E_m) was determined to be +335 mV versus NHE,[20] compared to the typical value of about +500 mV for P700 in other cyanobacteria. The photon energy used by P740 is lower (1.68 eV) than that of P700 (1.77 eV). However, the reducing power of P740* is equivalent to that of P700 because of the lower midpoint potential of P740.[20] It has been suggested that P740 might be an adaptation to the far-red light environments or an evolutionary intermediate between the red-absorbing oxygenic (P700 with chl *a*) and the far-red absorbing anoxygenic photosynthesis with Bchls.[21]

Laser spectroscopy, ENDOR, and FTIR studies indicated that the structure and environment of P740 are similar to those of P700. Time-resolved step-scan Fourier transform infrared (TRSS FT-IR) and visible (FT-vis) absorption difference spectra of a photosystem I particle from *A. marina* were presented by Hastings on a microsecond time scale.[22] The (P740$^+$−P740) IR spectrum band pattern was very similar to that of (P700$^+$−P700) from the cyanobacterium *Synechocystis sp.* PCC 6803. This evidence indicates that P740 is probably also a dimer that is similar to P700 except that it is a pair of chl *d* instead of chl *a* molecules. Extraction and reconstitution of the phylloquinone molecule were also performed in the photosystem I particle, and the function of quinone was assumed to be similar to that observed in other PS I complexes.[23]

On the basis of the information available at present, agreement has been reached on the fact that photosystem I in *A. marina* contains a dimer of chl *d* or more likely a heterodimer consiting of one molecule of chl *d* and one molecule of the epimer chl *d*′.[20,24] However, the pathway of chl *d* biosynthesis, the polypeptide arrangement of the antenna complexes and reaction centers, the energy transfer within the antenna, the trapping process from the antenna to the reaction center, and the electron-transfer kinetics within the reaction centers need to be further understood to better understand the mechanism of photosynthesis in this unique organism.

In this study, the photosystem I complex from *A. marina* was purified and further characterized by ultrafast transient difference absorption spectroscopy on the picosecond time scale as well as steady-state and time-resolved fluorescence spectroscopy. Our data provide more detailed information on the energy transfer and the excitation dynamics within the antenna and the trapping process in photosystem I.

Materials and Methods

Cell Culture. *A. marina* cell culture was a generous gift from Dr. S. Miyachi. Cells were grown in a modified K + ESM medium based on the methods of Miyashita[25] under dim light of 25 μeinstein m^{-2} s^{-1} at 28 °C with continuous moderate aeration. Cells were harvested at the late exponential phase.

Purification of Photosystem I Complex. Cells were washed with media and with the suspension buffer (20 mM (Bis-)Tris, pH = 7, 20% (w/v) glycerol, 10 mM $CaCl_2$, 10 mM NaCl, 2 mM $MgCl_2$, 2 mM Na_2EDTA, 2 mM benzamidine, and 2 mM phenylmethanesulfonyl fluoride (PMSF)). Cells were resuspended in the suspension buffer with 1 M sorbitol and 10% glycerol, kept on ice for 1 h, and then washed again with the suspension buffer without sorbitol. Cells were resuspended in the suspension buffer at a chlorophyll concentration greater than 0.1 mg mL^{-1} and were left on ice for 30 min. All centrifugation washes were carried out at 6000*g*. PMSF at 2 mM and 0.5 g mL^{-1} DNase I (Sigma) were added to the cell suspension and incubated for 15 min at 4 °C.

Cells were broken by passage through a French pressure cell three times at 20 000 psi. To ensure more complete cell breakage, a 50 mL sample was then treated using a Bead Beater (Biospec) with 25 mL of 0.1-mm diameter glass beads at 0 °C for 8−10 cycles, 20−30 s per cycle, with 5 min of cooling intervals between cycles. The beads were removed by 1000*g* centrifugation. The resulting supernatant liquid was centrifuged at 3000*g* for 10 min to remove unbroken cells. The chlorophyll *d* concentration in the supernatant was determined by the method given in ref 19.

To collect thylakoid membranes, the supernatant liquid was ultracentrifuged at 180 000*g* for 30 min, and the thylakoid membranes were washed free of phycobiliproteins with the suspension buffer. Thylakoid membranes were resuspended in the same buffer with the chlorophyll *d* concentration of 0.5−1 mg mL^{-1}. Solubilization with a mixed detergent (β-dodecylmaltoside/octylglucoside/zwittergen 3−14 = 6:3:1 w/w/w) was carried out on ice in the dark for 30 min. The ratio detergent/chlorophyll *d* was 10:1 w/w.

The solubilized thylakoid membrane suspension was loaded onto a 10−30% or 6−40% linear sucrose gradient in a buffer with the same components as the suspension buffer except with 0.03−0.04% β-DM and without glycerol and was ultracentrifuged in a SW 41 Ti rotor at 288000*g* for 18−20 h at 4 °C.

To purify the reaction center further, gel filtration by Sephacryl S-300 (10−15 cm long and ∼1 cm in diameter) was done at 4 °C on the photosystem I-enriched fractions generated from the sucrose gradient. Fractions were collected and reconcentrated for spectroscopy studies.

Spectroscopy. Steady-state absorption spectra were measured on a Shimadzu model UV-2501 UV−vis recording spectrophotometer.

Steady-state fluorescence measurements were performed on a Photon Technology International fluorescence spectrophotometer. The absorption of the samples was adjusted to ∼0.1 per cm at the Qy band. Photosystem I samples always contained 20 mM sodium ascorbate. The low-temperature (77 K) measurements were done with a variable-temperature liquid-nitrogen cryostat (Oxford Instruments, Inc.).

Single-photon counting time-resolved fluorescence on the picosecond time scale was performed on a locally built system described previously.[26] The excitation pulses were at 600 nm, with a 10-ps duration at a 7.6-MHz repetition rate. For these experiments, the sample absorption at the Qy peak was adjusted to 0.1 per cm. Sodium ascorbate was added to a final concentration of 20 mM. Decay traces were collected at multiple wavelengths between 650 and 790 nm. The data were analyzed with the locally written software asufit.

Difference absorption data on the millisecond time scale were measured on a transient absorption spectrophotometer as previously described.[27] *A. marina* photosystem I samples were suspended in the suspension buffer (pH 7), and the absorption was adjusted to 1.0 per cm at the Qy band (706−708 nm) and contained 20 mM ascorbate. Phenazinemethosulfate (PMS) (10 μM) was added to speed up the decay of P740$^+$. A decay curve was obtained at each wavelength by averaging the results of

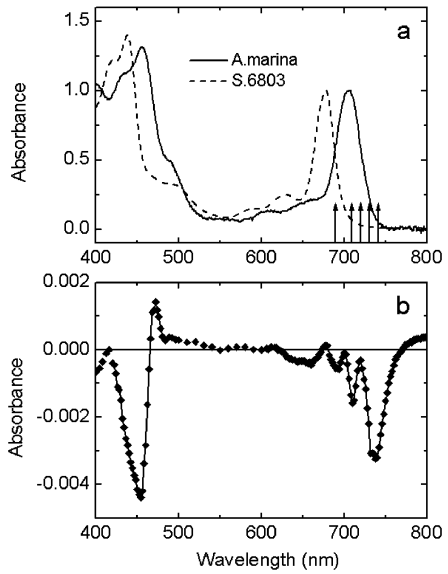

Figure 1. (a) Comparison of the absorption spectra of photosystem I from *Synechocystis sp*. PCC 6803 (- -) and *A. marina* (—). The former has a Qy absorption peak at 678 nm and a Soret band at 440 nm. The latter has a Qy peak at 707 nm and a Soret band at 456 nm. The arrows indicate the excitation wavelengths used in femtosecond transient absorption measurements: 690, 710, 720, 730, and 740 nm. (b) Laser-induced difference spectrum on the millisecond time scale of the photosystem I complex from *A. marina*.

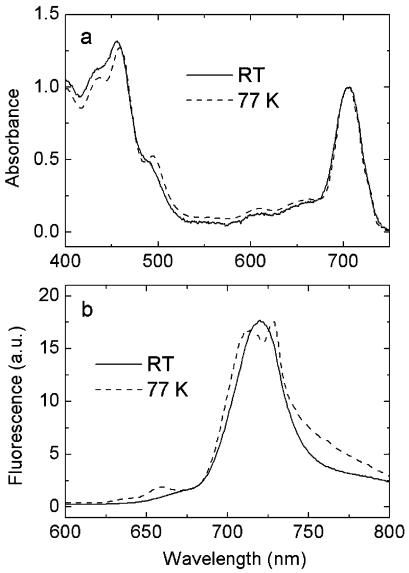

Figure 2. Steady-state spectra of the photosystem I complex measured at room temperature (—) and 77 K (- -) (a) absorption and (b) fluorescence with 456-nm excitation.

100 flashes. A difference spectrum at a given time after the flash was then constructed using all of these decay curves at each wavelength.

The femtosecond time scale laser system was an amplified KHz Ti−sapphire laser system (Clark-MXR, model CPA-1000) described previously.[28] Absorption difference spectra from 640 to 760 nm were obtained with a wavelength resolution of 1 nm and at various time delays. To investigate ultrafast excitation-energy transfer within the core antenna system, the sample was excited at selected wavelengths: 690, 710, 720, 730, and 740 nm with a spectral bandwidth of 5 nm. Global analysis was applied to each data matrix, and decay-associated spectra (DAS) were constructed after deconvolution of the observed kinetics with the excitation pulse and dispersion correction of the probe light.

For room-temperature measurements, the sample was loaded into a spinning wheel with an optical path length of 2.5 mm. The absorbance of the sample was adjusted to 1.5−1.6 in the spinning cell at the Qy absorption peak of 706 nm. The cell was rotated at a speed of 2 revolutions per second. Ascorbate (20 mM) and PMS (10 μM) were added to the sample. For measurements at 77 K, glycerol was added to the sample to a final composition of 1:2 (v/v). Then the sample was frozen to 77 K in the cryostat (see above).

Results and Discussion

Three major bands resolved from the sucrose gradient were collected and analyzed by SDS-PAGE and steady-state spectroscopy. The upper band is an antenna complex containing chlorophyll *d*, carotenoid, and protein; the middle band is a mixture of photosystem I monomers and photosystem II; the bottom band is primarily trimeric photosystem I.[19] This agrees with the results of previous studies by SDS-PAGE, Western blotting, and N-terminal amino acid sequence analysis.[19,20]

Figure 1a compares the isolated photosystem I complexes from *Synechocystis sp.* PCC 6803 and *A. marina*. Overall, the two spectra are similar in shape, but there are obvious differences between them. *Synechocystis sp.* PCC 6803 is a typical cyanobacterium, with chl *a* as its major pigment with a Qy peak at 678 nm and a Soret peak at 440 nm. However, the *A. marina* photosystem I has a Qy peak at 707 nm and a Soret peak at 456 nm. It also has a broader shoulder on the red side (over 710 nm) and another shoulder hidden in the edge of the Soret band at 490 nm. Both peaks are broader and less symmetric for *A. marina* than for *Synechocystis* 6803. These differences are due to the fact that chl *d* is its major pigment. The arrows in Figure 1a indicate the excitation wavelengths used in the femtosecond transient absorption measurements (see below). Figure 1b shows the millisecond time scale light-induced difference spectrum for photooxidation of P740 (see below). The spectrum shown in Figure 1b agrees well with the spectrum presented by Hu et al.[20] This spectrum has two major bleaching peaks—one at 740 nm, which led to the designation P740 (versus the 700-nm peak of regular P700), and another one at 455 nm (versus the 430-nm peak of regular P700). Minor bleaching peaks are observed at 650, 690, and 710 nm. The positive regions of the difference spectrum are at 475 nm and above 765 nm. The $P740^+$ decay time was 40 ms with only ascorbate added and was shortened by increasing the amount of PMS.

The absorption spectrum of photosystem I from *A. marina* was also measured at 77 K (Figure 2a). At low temperature, several additional spectral details were revealed. New peaks at 442 and 497 nm and small bumps at 610 and 660 nm as well as a tiny hump at 740 nm were observed in the 77 K profile. Also, the Soret peak shifts from 458 nm at room temperature to 461 nm at 77 K. The low-temperature spectra reveal the different pools of chl *d* within the photosystem I complex, especially the cluster at 740 nm. The majority of the antenna pigments absorbs at 708 nm.

Steady-State and Time-Resolved Fluorescence. Steady-state fluorescence was measured at both room temperature and 77 K (Figure 2b). In both cases, the sample was excited at 456 nm, which is both the Soret absorption peak of photosystem I (Figure 2a) and the major bleaching band of the difference absorption spectrum of photosystem I (see below). At room temperature, the emission peak is at 722 nm. This was always observed to be the dominant emission band, independent of the excitation

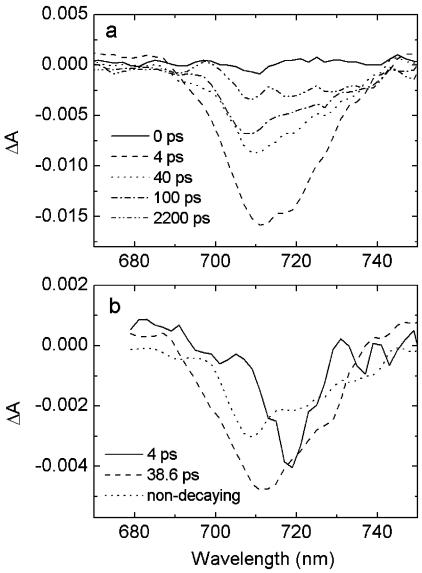

Figure 3. (a) Time-resolved spectra (TRS) and (b) decay-associated spectra (DAS) of photosystem I with low excitation intensity at 720 nm. The sample contained 20 mM sodium ascorbate and 10 μM PMS. The time-resolved spectra are at 0 ps (—), 4 ps (- -), 40 ps (••), 100 ps (-•-) and 2200 ps (-••-). Three DAS components are shown: 4 ps (—), 38.6 ps (- -), and the nondecaying component (••).

wavelength. At 77 K, the emission spectrum shows two peaks at 715 and 730 nm. Two other small shoulders at 638 and 660 nm were also observed. On the red side, from 740 to 820 nm, the emission increases significantly, although no separate band was observed. At room temperature, on the contrary, this feature was not observable, probably due to thermal broadening.

Time-correlated single-photon-counting fluorescence was measured on a photosystem I sample at room temperature after excitation at 600 nm (data not shown). Decay curves were recorded in 10-nm intervals from 650 to 790 nm and were fit with lifetimes of 32, 470, and 2526 ps along with corresponding relative amplitudes of 94.8, 3.52, and 1.66. The major decay component, 32 ps, is thought to be the trapping time for excitation energy to go into the reaction center. The long components, considered nondecaying on this time scale, are attributed to the excitation energy decay in uncoupled antenna pigments.

Transient Absorption Spectra. Transient absorption spectra were carried out on the millisecond, picosecond, and femtosecond time scales. Before each measurement on the picosecond and femtosecond time scales, the difference absorption spectrum of the photosystem I complex was measured on the millisecond time scale at room temperature (Figure 1b).

Transient Difference Absorption Spectra on the Picosecond Time Scale. The photosystem I sample was examined by the picosecond pump−probe experiment. The sample was excited at 720 nm. The light-induced difference spectra were scanned from −20 to 2000 ps in step sizes of 4 and 100 ps per step. The excitation intensity was first adjusted to a low level and was increased in some experiments. A "low" excitation intensity is defined in such a way that less than 1 photon is absorbed per RC to avoid annihilation. The low excitation with finer time resolution gives a trapping time free from any annihilation effects. The high-intensity excitation is carried out for the purpose of seeking the charge-separated species on the longer time scale.

Figure 3a shows the time-resolved spectra (TRS) with low excitation intensity. Pumped at 720 nm, the excitation energy is rapidly transferred to 710 nm within 4 ps followed by a partial recovery of the bleaching. The long-lived bleaching shows a weak band around 740 nm, which is presumably due to the formation of $P740^+$. The spectrum observed under high excitation intensity shows a very similar spectral profile.

The decay-associated spectra (DAS) are best fit with three components (Figure 3b). The fast component has a lifetime of 4 ps and represents the initial bleaching at the excitation wavelength and the fast energy transfer within the antenna system. The 40-ps component is thought to be the trapping time, in good agreement with the 32-ps value observed in the time-resolved fluorescence results. It has a single negative peak at 710 nm and a shoulder at 725 nm. The nondecaying component has a broad negative band from 680 to 750 nm. The major peak still resides at 710 nm. Around 740 nm, the amplitude is negative, but no pronounced band was resolved. Several different experiments were carried out in an attempt to obtain a better-resolved $P740^+$ spectrum on the picosecond time scale by increasing the sample optical density, improving the sample purity, increasing the excitation intensity, and scanning for long times up to 4 ns (Figure 3a), and the results were found to be reproducible with all of these considerations and invariable with all of the different fitting parameters. The nondecaying component is always dominated by a broad band around 710 nm and is also essentially identical to the time-resolved spectrum at very late time (high excitation intensity data, not shown). There are several possibilities for the identity of the species that leads to the 710-nm band that lives for nanoseconds or longer. It may be an unattached antenna complex that is not able to transfer to P740. Another possibility is that the 710-nm bleaching is due to a chl *d* molecule that serves as a mainstream electron acceptor but has a lifetime longer than anticipated on the basis of other cyanobacterial photosystem I complexes. Finally, it could be due to a population of photosystem I complexes that for unknown reasons are not capable of normal electron transfer, possibly because of some damage during purification. Extensive purification of the sample by various columns did not reduce this long-lived 710-nm component. In addition, it was still observed when excitation was at 740 nm. Both of these facts strongly suggest that it is not a simple contaminant of free pigments or disconnected antenna complexes. Although we cannot at this time rule out the second possibility, it seems unlikely on the basis of comparisons to other photosystem I systems. The last possibility seems to be the most likely, but there is no independent evidence for this proposed large amount of sample heterogeneity. Additional work over a wider range of time scales will be necessary to resolve this issue.

Transient Difference Absorption Spectra on the Femtosecond Time Scale. A set of experiments were carried out to explore the excitation dynamics in the core antenna. For measurements of selective excitation of the core antenna, the excitation wavelengths (shown in Figure 1b) were chosen according to the different pools of pigments in the photosystem I complex: the pool of chl *d* that absorbs around 740 nm, which was revealed by the 77 K absorption spectrum; the bulk antenna absorbing at 710 nm; and the other clusters of chl *d* absorbing at 720 and 730 nm, which results in the asymmetric shape of the photosystem I Qy band in the absorption spectrum. Another pool of pigments on the blue side of the absorption spectrum was also studied by the 690-nm excitation.

Figure 4 shows the spectral evolution from 0.3 ps up to 5 ps with excitation at various wavelengths. For the 690-nm excitation (Figure 4a), the initial spectrum experienced a red shift.

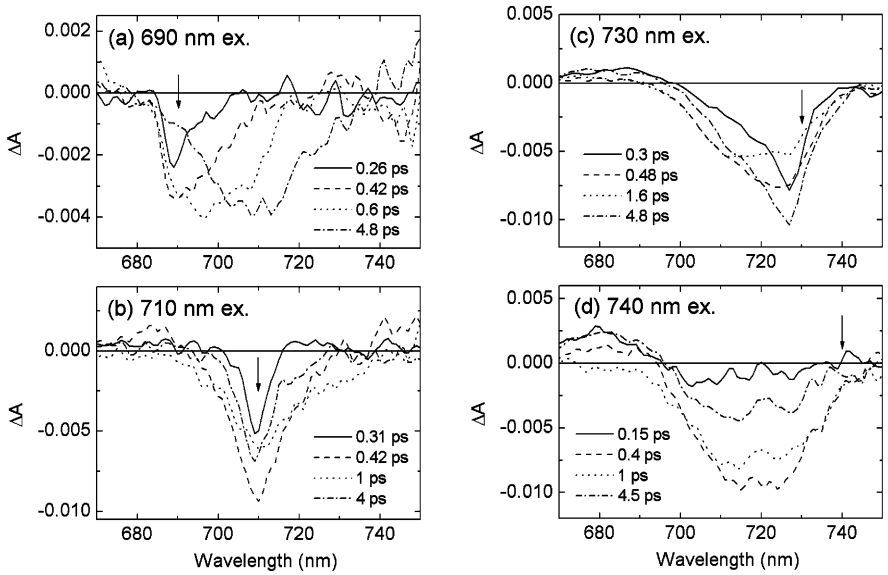

Figure 4. Time-resolved spectra (TRS) with (a) 690-nm excitation, (b) 710-nm excitation, (c) 730-nm excitation, and (d) 740-nm excitation. In panel a, traces are shown at 0.26 ps (—), 0.42 ps (- -), 0.6 ps (••), and 4.8 ps (-•-). In panel b, traces are shown at 0.31 ps (—), 0.42 ps (- -), 1 ps (••), and 4 ps (-•-). In panel c, traces are shown at 0.3 ps (—), 0.48 ps (- -), 1.6 ps (••), and 4.8 ps (-•-). In panel d, traces are shown at 0.15 ps (—), 0.4 ps (- -), 1 ps (••), and 4.5 ps (-•-).

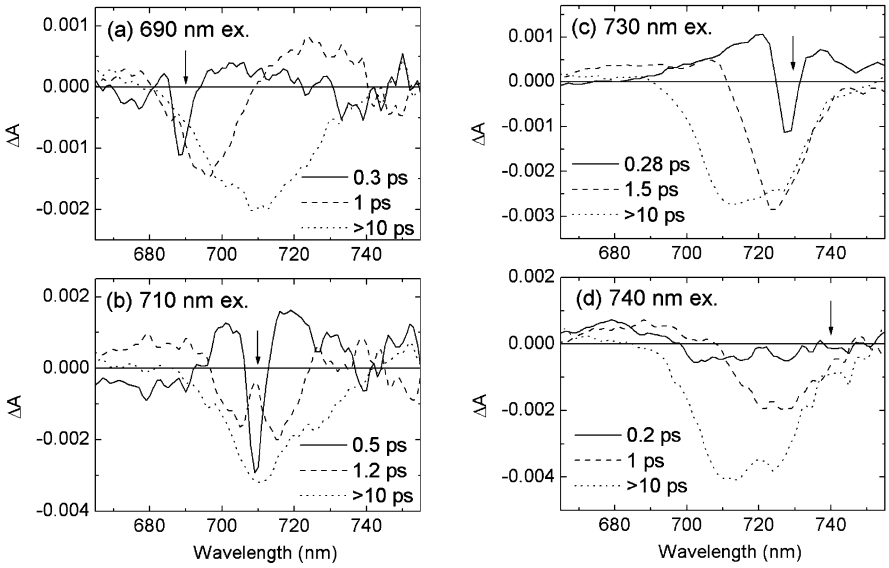

Figure 5. Decay associated spectra (DAS) with (a) 690-nm excitation, (b) 710-nm excitation, (c) 730-nm excitation, and (d) 740-nm excitation. In panel a, DAS are shown with times of 0.3 ps (—), 1 ps (- -) and >10 ps (••). In panel b, DAS are shown with times of 0.5 ps (—), 1.2 ps (- -), and >10 ps (••). In panel c, DAS are shown with times of 0.28 ps (—), 1.5 ps (- -), and >10 ps (••). In panel d, DAS are shown with times of 0.2 ps (—), 1 ps (- -), and >10 ps (••).

At 0.3 ps, it is very asymmetric, with the peak at 690 nm and with a small amount of stimulated emission at 685 nm and also on the red side at 705 nm. The band broadens on the red side and becomes more symmetric at 5 ps. These changes illustrate a downhill energy transfer from the pool of chl *d* at 690 nm to those at longer wavelengths.

For the 710-nm excitation (Figure 4b), the situation is somewhat different. The 0.3-ps spectrum is sharp and symmetric. From 0.3 to 1 ps, the spectrum is broadened on both sides, and the bleaching increases at the same time. The decay begins at 1 ps. The resulting 4-ps spectrum is very broad and overall symmetric, and it still has the peak at 710 nm but with a shoulder at 730−740 nm. These features indicate energy transfer from the bulk antenna absorbing at 710 nm to all other pools of chlorophylls but with preference to lower-energy pigments.

For 730-nm excitation (Figure 4c), which is on the red side of the Qy peak, a similar energy-transfer process to that of 690-nm excitation was seen. But this transfer is in the opposite direction, that is, uphill from 730 to 710 nm.

For 740-nm excitation (Figure 4d), which is where the special pair absorbs, an interesting feature is noticed. The 0.15-ps spectrum is already very broad, from 700 to 740 nm, with maximum bleaching at 705 nm. There is not a sharp band at 740 nm, which indicates strong excitonic coupling of the pigments in the reaction center P740. The spectral bleaching keeps rising from 0.15 to 4.5 ps and shifts to the red up to 725 nm. The 4.5-ps spectrum is quite symmetric, centered at 720 nm. It then evolves quickly to 710 nm.

The decay-associated spectra with various wavelengths of excitation are shown in Figure 5. The data are best fit with three components. The fastest component has a lifetime of 200−500

fs. Its shape is strongly excitation wavelength-dependent. The second component has a lifetime of 1−1.5 ps, also indicating the further excitation energy equilibration. The slowest component, with a lifetime of ∼40 ps, is due to the trapping of excitation energy into the reaction center. This component is excitation wavelength-independent and has a similar shape to that of the 40-ps component measured on the 2000-ps scale. The nondecaying component on this ultrafast time scale corresponds to the middle component in the longer scan. In some analyses, this 40-ps time was fixed in the global analysis. It generated the same DAS as with the program freely running without any fixed lifetimes.

Compared to the result of *Synechosystis sp*. PCC 6803, our data show similar uphill or downhill energy transfers in the excitation equilibration process.[9,10] However, in *A. marina*, the excitation is quickly localized on 710-nm absorbing pigments, and there is no indication for a pool of "red" pigments whose energy is lower than that of the special pair. Although most cyanobacteria appear to contain these long-wavelength pigments, some organisms such as *Gloeobacter* lack them.[29] The function of these long-wavelength pigments is still not well understood.

Conclusions

Photosystem I particles from *A. marina* were isolated and characterized using ultrafast spectroscopy. The inhomogeneous broadening reflects the existence of different pools of chl *d* in the complex. Absorbance difference spectra on the picosecond time scale were measured with different excitation intensities, at various excitation wavelengths, and on different time scales. The trapping of excitation energy into the reaction center was found to occur at 40 ps and was confirmed by time-resolved fluorescence. From the selective excitation of the core antenna, downhill or uphill energy transfer was observed at early times, with excitations rapidly localized on pigments absorbing at 710 nm. The initial spectral shape is excitation wavelength-dependent, but they all reach an excited-state equilibrium, independent of the excitation wavelength, within several picoseconds. Three components were resolved in the DAS. The subpicosecond and 1-ps components are attributed to the equilibration among antenna pigment pools. The 40-ps component is due to trapping. There is no evidence of the existence of red pigments at wavelengths longer than the primary donor. The existence of the 710-nm pigment form appears to be unique for *A. marina*. Since no structural information is available for this species, further experiments are needed to identify these pigments.

After the submission of this paper, a paper was published on a similar topic using the same organism.[30] Although there are some differences in experimental conditions and results, most of the observations in this paper are consistent with our work.

Acknowledgment. This work was supported by the U.S. National Science Foundation (grant no. MCB-0091250). We thank Dr. Qiang Hu for valuable discussions.

References and Notes

(1) Blankenship, R. E. *Molecular Mechanisms of Photosynthesis*; Blackwell Science: Oxford, U.K. 2002.

(2) *The Molecular Biology of Cyanobacteria*; Bryant, D. A., Ed.; Kluwer Academic Press: Dordrecht, The Netherlands, 1994.

(3) Turner, S. *Plant Syst. Evol., Suppl.* **1997**, *11*, 13.

(4) Miyashita. H.; Ikemoto, H.; Kurano, N.; Adachi, K.; Chihara, M.; Miyachi, S. *Nature (London)* **1996**, *383*, 402.

(5) Miyashita, H.; Adachi, K.; Kurano, N.; Ikemoto, H.; Chihara, M.; Miyachi, S. *Plant Cell Physiol.* **1997,** *38*, 274.

(6) Wu, X.; Tang, H.; Wang, Y.; Chitnis, P. R. *Biochim. Biophys. Acta* **2001**, *1507*, 32.

(7) Jordan, P.; Fromme, P.; Witt, H. T.; Klukas, O.; Saenger, W.; Krauβ, N. *Nature (London)* **2001**, *411*, 909−917.

(8) Byrdin, M.; Jordan, P.; Krauss, N.; Fromme, P.; Stehlik, d.; Schlodder, E. *Biophys. J.* **2002**, *83*, 433.

(9) Melkozernov, A. N. *Photosynth. Res.* **2001**, *70*, 129.

(10) Gobets, B.; van Grondelle, R. *Biochim. Biophys. Acta* **2001**, *1507*, 80.

(11) Brettel, K.; Leibl, W. *Biochim. Biophys. Acta* **2001**, *1507*, 100.

(12) Trissl, H. *Photosynth. Res.* **1993**, *35*, 247.

(13) Pålsson, L. O.; Flemming, C.; Gobets, B.; van Grondelle, R.; Dekker, J. P.; Schlodder, E. *Biophys. J.* **1998**, *74*, 2611−2622.

(14) Melkozernov, A. N.; Lin, S.; Blankenship, R. E. *Biochemistry* **2000**, *39*, 1489−1498.

(15) Schiller, H.; Senger, H.; Miyashita, H.; Miyachi, S.; Dau, H. *FEBS Lett*. **1997**, *410*, 433−436.

(16) Boichenko, V. A.; Klimov, V. V.; Miyashita, H.; Miyachi, S. *Photosynth. Res.* **2000**, *65*, 269−277.

(17) Marquardt, J.; Senger, H.; Miyashita, H.; Miyachi, S.; Mörschel, E. *FEBS Lett.* **1997**, *410*, 428−432.

(18) Hu, Q.; Marquardt, J.; Iwasaki, I.; Miyashita, H.; Kurano, N.; Mörschel, E.; Miyachi, S. *Biochim. Biophys. Acta* **1999**, *1412*, 250−261.

(19) Chen, M.; Quinnell, R. G.; Larkum, A. W. D. *FEBS Lett.* **2002,** *514*, 149−152.

(20) Hu, Q.; Miyashita, H.; Iwasaki, I.; Kurano, N.; Miyachi, S.; Iwaki, M.; Itoh, S. *Proc. Natl. Acad. Sci. U.S.A.* **1998**, *95*, 13319−13323.

(21) Blankenship, R. E.; Hartman, H. *Trends Biochem. Sci.* **1998**, *23*, 94−97.

(22) Hastings, G. *Appl. Spectrosc.* **2001**, *55*, 894−900.

(23) Itoh, S.; Iwaki, M.; Noguti, T.; Kawamori, A.; Mino, H. *PS2001 Proceedings, 12th International Congress on Photosynthesis*; CSIRO Publishing: Collingwood, Victoria, Australia, 2001; S6−028, 1−4.

(24) Akiyama, M.; Miyashita. H.; Kise, H.; Watanabe, T.; Miyachi, S.; Kobayashi, M. *Anal. Sci.* **2001**, *17*, 205.

(25) Miyashita. H. *J. Mar. Biotechnol*. **1995**, *3*, 136−139.

(26) Causgrove, T. P.; Brune, D. C.; Olsen, J. M.; Blankenship, R. E. *Photosynth. Res.* **1990**, *25*, 1−10.

(27) Kleinherenbrink, F. A. M.; Chiou, H.-C.; LoBrutto, R.; Blankenship, R. E. *Photosynth. Res.* **1994**, *41*, 115−123.

(28) Mi, D.; Lin, S.; Blankenship, R. E. *Biochemistry* **1999**, *38*, 15231−15237.

(29) Mimuro, M.; Ookubo, T.; Takahashi, D.; Sakawa, T.; Akimoto, S.; Yamazaki, I.; Miyashita, H. *Plant Cell Physiol.* **2002**, *43*, 587−594.

(30) Kumazaki, S.; Abiko, K.; Ikegami, I.; Iwaki, M.; Itoh, S. *FEBS Lett.* **2002**, *530*, 153−157.